Transport properties and magnetic-field-induced localization in the misfit cobaltite $[Bi_2Ba_{1.3}K_{0.6}Co_{0.1}O_4]^{RS}[CoO_2]_{1.97}$ single crystal

2008 J. Phys.: Condens. Matter 20 215221

(http://iopscience.iop.org/0953-8984/20/21/215221)

J. Phys.: Condens. Matter **20** (2008) 215221 (8pp) doi:10.1088/0953-8984/20/21/215221

Transport properties and magnetic-field-induced localization in the misfit cobaltite $[Bi_2Ba_{1.3}K_{0.6}Co_{0.1}O_4]^{RS}[CoO_2]_{1.97}$ single crystal

X G Luo, H Chen, G Y Wang, G Wu, T Wu, L Zhao and X H Chen[1]

Hefei National Laboratory for Physical Science at Microscale and Department of Physics, University of Science and Technology of China, Hefei, Anhui 230026, People's Republic of China

E-mail: chenxh@ustc.edu.cn

Received 9 January 2008
Published 24 April 2008
Online at stacks.iop.org/JPhysCM/20/215221

Abstract

Resistivity under magnetic field, thermopower and Hall coefficient are systematically studied for the $[Bi_2Ba_{1.3}K_{0.6}Co_{0.1}O_4]^{RS}[CoO_2]_{1.97}$ single crystal. In-plane resistivity ($\rho_{ab}(T)$) shows metallic behavior down to 2 K with a T^2 dependence below 30 K, while out-of-plane resistivity ($\rho_c(T)$) shows metallic behavior at high temperature and a thermal activation semiconducting behavior below about 12 K. The striking feature is that magnetic field induces a $\ln(1/T)$ diverging behavior in both ρ_{ab} and $\rho_c(T)$ at low temperature. The positive magnetoresistance (MR) could be well fitted by the formula based on multiband electronic structure. The $\ln(1/T)$ diverging behavior in ρ_{ab} and $\rho_c(T)$ could arise from the magnetic-field-induced 2D weak localization or spin density wave.

1. Introduction

Triangular cobaltites have attracted significant interest for their promising application prospect as thermoelectrical materials and their complex physical properties as strongly correlated electron systems [1–4]. The complex physical properties include the unconventional superconductivity in water-intercalated $Na_{0.35}CoO_2$ [5], temperature-dependent Hall effect [3, 6], large negative magnetoresistance (MR) in $(Bi, Pb)_2M_2Co_2O_y$ (M = Sr and Ca) and $Ca_3Co_4O_9$ [2, 6, 7], large thermopower (TEP) with low resistivity [1, 2], complicated magnetic structure [8–10], etc. These triangular cobaltites have the common structural unit of a CdI_2-type hexagonal $[CoO_2]$ layer, which is composed of edge-sharing CoO_6 octahedra. Among them, the so-called misfit cobaltites $Bi_2M_2Co_2O_y$ (M = Ca, Sr and Ba) [11] and $Ca_3Co_4O_9$ [2] are constructed by the alternative stacking rock-salt- (RS-) type blocks and $[CoO_2]$ layers. The two sublattices share common a- and c-lattice parameters, but possess different b-lattice lengths, causing a misfit along the b-axis with a misfit ratio b_{RS}/b_H (b_{RS} and b_H are the b-lattice parameters for RS and hexagonal sublattices, respectively). In $Bi_2M_2Co_2O_y$ (M = Ca, Sr and Ba), the quadruple RS block is composed of two deficient [BiO] layers sandwiched by two [MO] layers [11]. For M = Ba, commensurate modulation along b-axis between RS and hexagonal sublattices with $b_{RS}/b_H = 2.0$ was found [12], in contrast to the incommensurate modulation in other misfit cobaltites. Metallicity increases with increasing ionic radii from Ca to Ba [6, 7, 12], and the MR at low temperature also changes sign from negative in Ca and Sr compounds [6, 7] to positive in Ba compounds [12]. It has been found by us that there coexist large negative and positive contributions to the nonmonotonic magnetic-field-dependent MR in Pb-doped $Bi_2Sr_2Co_2O_y$ [13]. Spin-dependent charge transport has been taken into account for understanding the large negative MR in Sr and Ca compounds, but the large positive MR in Ba compounds has not been fully understood. In a polycrystalline $Bi_2Ba_2Co_2O_y$ sample, Hervieu *et al* reported that the positive isothermal MR exhibits a linear H dependence. They compared the behavior in Ba compounds with MR in Sr_2RuO_4 and heavy-fermion-like oxide LiV_2O_4 to

[1] Author to whom any correspondence should be addressed.

understand the positive MR [12]. However, the origin of large positive MR was not settled; further work, especially on single crystals, is required to understand this anomalous positive MR.

In this paper, a K-doped $Bi_2Ba_2Co_2O_y$ single crystal was grown through the flux method. The single crystal shows metallic resistivity in the ab plane down to 2 K, while it exhibits a weak thermal activation behavior along the c-axis at low temperature. Magnetic field induces a $\ln(1/T)$ diverging behavior at low temperature in $\rho_{ab}(T)$ and $\rho_c(T)$. The positive MR can be interpreted by the multiband electronic structure. The $\ln(1/T)$ diverging behavior in $\rho_{ab}(T)$ may be ascribed to the magnetic-field-induced 2D weak localization or spin density wave (SDW).

2. Experimental procedures

Bi–Ba–Co–O single crystals were grown by the solution method using K_2CO_3–KCl fluxes. Starting materials Bi_2O_3, $BaCO_3$ and Co_3O_4 were mixed in a proportion of Bi:Ba:Co = 2:2:2 with a total weight of 4 g. The powders were heated at 800 °C for 10 h. Then the prepared $Bi_2Ba_2Co_2O_y$ was mixed with a mixture of KCl and K_2CO_3 with a molar proportion of 1:4 (20.5 g), which was loaded in an aluminum crucible having 30 ml volume. The solute concentration was about 1.5 mol%. A lidded crucible was used to prevent the solution from evaporating and to grow crystals under stable conditions. The mixture was melted at 950 °C for 20 h, and then slowly cooled down to 600 °C at a rate of 5 °C h^{-1}. The single crystals were separated from the melt by washing with distilled water. The crystals were large thin platelets and black in color. Typical dimensions of the crystals are $5 \times 5 \times 0.05$ mm^3.

Single crystals were characterized by electron diffraction (ED) and x-ray diffraction (XRD) using Cu Kα radiation, respectively. The actual chemical composition of the single crystals was determined by the inductively coupled plasma (ICP) atomic emission spectroscopy (AES) (ICP-AES) technique and the x-ray energy dispersive spectrum (EDS). The obtained results from ICP-AES and EDS were almost consistent, Bi:Ba:K:Co = 2:1.3:0.6:2.1.

Susceptibility was measured using a SQUID magnetometer (MPMS-7XL, Quantum Design). Electrical transport was measured using the alternating current (ac) four-probe method with an ac resistance bridge system (Linear Research; LR-700P). The Hall effect is measured by the four-terminal ac technique. To eliminate the offset voltage due to the asymmetric Hall terminals, the magnetic field was changed from −5 to 5 T and the Hall voltage was calculated to be $\{V(H) - V(-H)\}/2$, where V is the voltage between the Hall probes. The dc magnetic field for MR measurements is supplied by a superconducting magnet system (Oxford Instruments). Thermoelectric power (TEP) was measured using the steady-state technique.

3. Experimental results

3.1. Structural characterization

XRD pattern shown in figure 1(a) indicates that the single crystals have perfect c-orientation with the c-axis lattice

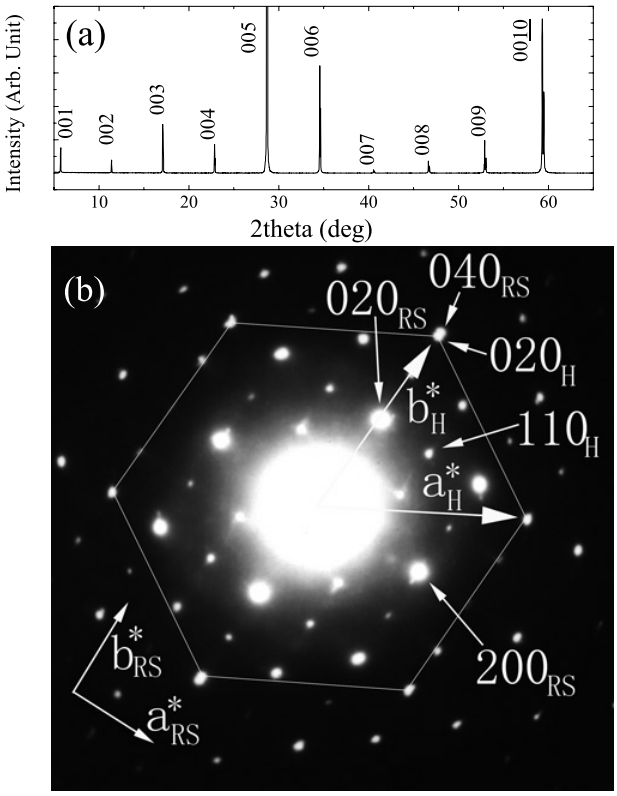

Figure 1. (a) X-ray diffraction pattern; (b) [001] electron diffraction pattern for the $[Bi_2Ba_{1.3}K_{0.6}Co_{0.1}]^{RS}[CoO_2]_{1.97}$ single crystal.

parameter of 15.55 Å, larger than that in the undoped polycrystalline sample (15.44 Å) [12], consistent with the substitution of the larger K^+ for the Ba^{2+} ion ($r_{K^+_{VI}} = 1.38$ Å, $r_{Ba^{2+}_{VI}} = 1.36$ Å) [14]. The [001] ED pattern shown in figure 1(b) is similar to that of the undoped sample reported by Hervieu *et al* [12] except that the reflection of $(020)_H$ visibly separates from that of $(040)_{RS}$ (where H and RS refer to the hexagonal and RS sublattices, respectively). In-plane lattice parameters can be estimated from the [001] ED pattern. The **a** and **b** parameters of the RS sublattice are larger than those in the undoped polycrystalline sample. a_{RS} and b_{RS} are 4.905 and 5.640 Å for the undoped polycrystalline sample, while 5.031 and 5.683 Å for the present single crystal, respectively. This is due to the substitution of the larger K^+ for the Ba^{2+} ion. Along the **a** axis, we obtain $a_{RS} = \sqrt{3}a_H$ ($a_H = 2.907$ Å), indicating that the RS and H subsystems share a common a-axis lattice parameter. Along the **b** axis, however, an incommensurate modulation with the misfit ratio $b_{RS}/b_H = 1.97$ ($b_H = 2.88$ Å) can be obtained, indicating that $\mathbf{b}_{RS}$ and $\mathbf{b}_H$ axes are collinear but aperiodic. This is in contrast to the commensurate modulation along the **b** direction in the undoped polycrystalline sample ($b_{RS}/b_H = 2$) [12]. Therefore, the structural formula of the present compound could be written as $[Bi_2Ba_{1.3}K_{0.6}Co_{0.1}O_4]^{RS}[CoO_2]_{1.97}$.

3.2. Magnetic susceptibility

The temperature dependences of the magnetic susceptibility (χ) recorded at $H = 1000$ Oe with H perpendicular to the

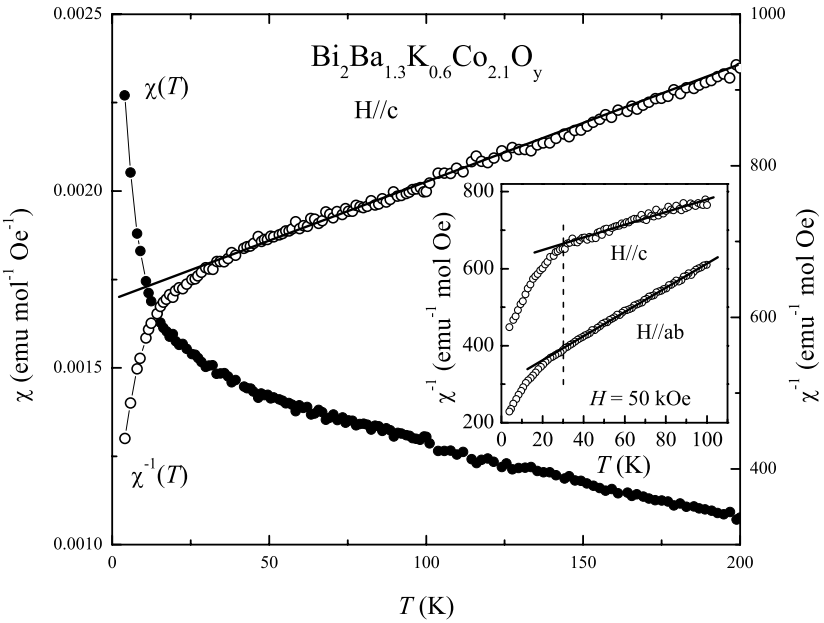

Figure 2. The temperature dependence of the magnetic susceptibility and its inverse, collected at 0.1 T with H parallel to the c-axis. The inset shows the inverse magnetic susceptibility for H parallel to both the c-axis and the ab-plane, in which a downturn from the high-temperature linear part can be observed, just as in the main pattern.

ab plane and its inverse (χ^{-1}) are shown in figure 2. The high-temperature linear χ^{-1} indicates a paramagnetic state. Below about 30 K, however, there exists an abnormal decrease in χ^{-1}, suggesting a short-range magnetic order. Another interpretation for the deviation of χ^{-1} at 30 K could be the formation of an SDW. As in previous reports for $Bi_2Ca_2Co_2O_y$ (structurally, $[Ca_2Bi_{1.7}Co_{0.3}O_4]^{RS}[CoO_2]_{1.67}$) [7, 10], the temperature where the low-temperature χ^{-1} deviates down from the high-temperature linear part is almost the same as that where the SDW begin to form as detected by μSR. Therefore, the downturn of χ^{-1} at about 30 K from the high-temperature linear part in the present crystal may suggest the appearance of the SDW. But Sugiyama *et al* [10] reported that there is no SDW down to 1.8 K in the undoped polycrystalline sample, so the μSR experiment is required to confirm whether there exists an SDW in the present crystal. The curves registered at $H = 50$ kOe with H both parallel and perpendicular to the ab plane are shown in the inset. The deviation from the high-temperature linear χ^{-1} still exists around 30 K.

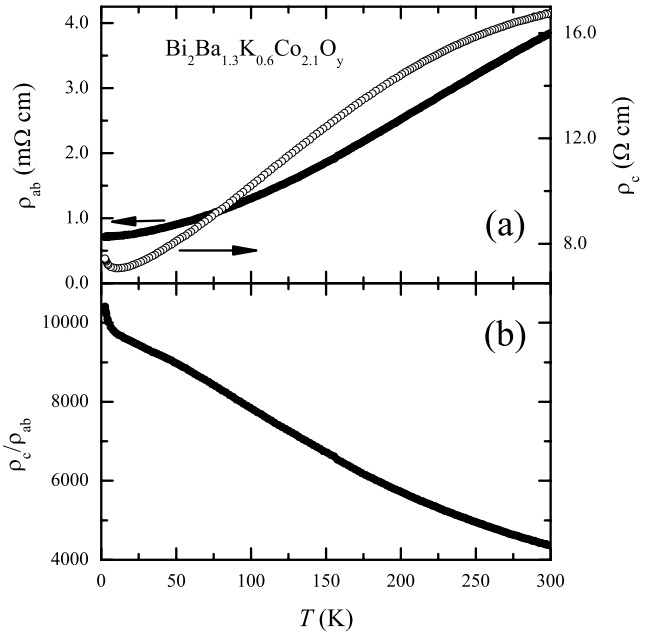

Figure 3. (a) Temperature dependence of in-plane and out-of-plane resistivity; (b) temperature dependence of resistivity anisotropy ρ_c/ρ_c for the $[Bi_2Ba_{1.3}K_{0.6}Co_{0.1}O_4]^{RS}[CoO_2]_{1.97}$ single crystal.

3.3. Resistivity, Hall coefficient and thermopower

Figure 3(a) shows the temperature dependence of the in-plane and out-of-plane resistivity ($\rho_{ab}(T)$ and $\rho_c(T)$) for the $[Bi_2Ba_{1.3}K_{0.6}Co_{0.1}O_4]^{RS}[CoO_2]_{1.97}$ single crystal. $\rho_{ab}(T)$ shows metallic behavior down to 2 K. This contrasts with the semiconducting behavior below 80 K in the undoped polycrystalline sample [12]. It suggests that K doping on the Ba sites induces excess charge carriers into the system. Figure 4(a) indicates that the metallic in-plane resistivity below 30 K follows T^2-dependence, indicative of strong electron correlation in the crystal. Such behavior is similar to that observed in $Na_{0.7}CoO_2$ [4]. However, out-of-plane resistivity shows a weak semiconducting behavior below 12 K. Figure 4(b) indicates that the weak semiconducting behavior obeys thermal activation behavior with an activation energy of 0.013 meV. At high temperature, the out-of-plane resistivity shows metallic behavior up to room temperature. No incoherent-to-coherent behavior is observed in this crystal, contrasting with the Pb-doped $Bi_2Ba_2Co_2O_y$ [15], in which $\rho_{ab}(T)$ is metallic down to 2 K, while $\rho_c(T)$ shows

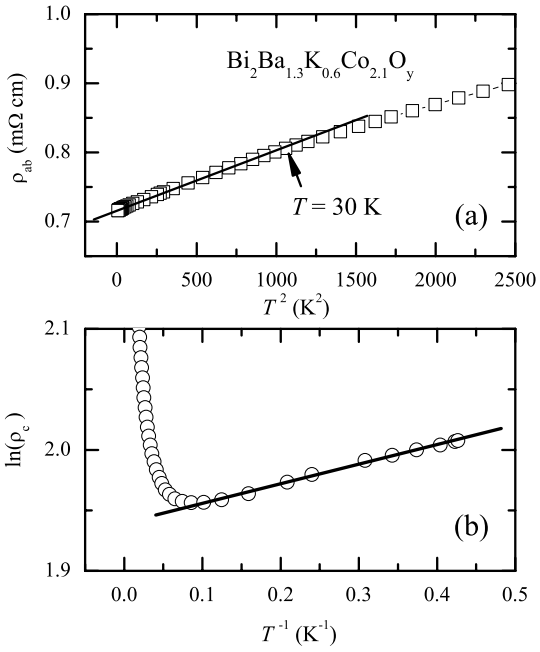

Figure 4. (a) T^2 dependence of the in-plane resistivity below 50 K; (b) plot of $\ln(\rho_c)$ versus $1/T$ for the $[Bi_2Ba_{1.3}K_{0.6}Co_{0.1}O_4]^{RS}[CoO_2]_{1.97}$ single crystal.

a incoherent-to-coherent transition at about 180 K with decreasing temperature. It should be pointed out that metallic behavior in $\rho_{ab}(T)$ and semiconducting-like behavior in $\rho_c(T)$ is similar to the case of an underdoped sample in the high-T_c cuprates, in which $\rho_{ab}(T)$ shows metallic behavior, while $\rho_c(T)$ becomes divergent at low temperature [16]. This behavior is ascribed to opening of a pseudogap. However, similar behavior in the $[Bi_2Ba_{1.3}K_{0.6}Co_{0.1}O_4]^{RS}[CoO_2]_{1.97}$ single crystal cannot be understood so far. Figure 3(b) shows the temperature dependence of the anisotropy ρ_c/ρ_{ab}. ρ_c/ρ_{ab} is larger than $\sim 10^3$ in the whole temperature range, suggesting a highly anisotropic electronic structure. The anisotropy ρ_c/ρ_{ab} increases with decreasing temperature, similar to that observed in the $(Bi, Pb)_2Sr_2Co_2O_y$ crystals [13]. Strongly temperature-dependent anisotropy indicates that the scattering mechanism is different between in plane and along the c-axis, suggesting a quasi-two-dimensional electronic structure [16].

Figure 5(a) shows the temperature dependence of the Hall coefficient (R_H) of the crystal. R_H is positive and shows strong temperature dependence. Charge carrier concentration can be estimated from R_H at room temperature to be 1.33×10^{21} cm^{-3}, one-third of that observed in $Na_{0.7}CoO_2$ [3] and twice that observed in $Ca_3Co_4O_9$ [17]. In figure 5(b), it is found that the high-temperature R_H is proportional to T^2, different from the linear temperature-dependent R_H in $Na_{0.7}CoO_2$ [3]. This suggests different electronic structure between the present misfit-layered cobaltite and Na_xCoO_2. Although ρ_{ab} is metallic down to 2 K, R_H shows an upturn below about 70 K with decreasing temperature. Similar behavior in Hall coefficient has been observed in $(Bi, Pb)_2Sr_2Co_2O_y$ single crystals [6], in which the upturn of R_H at low temperature is ascribed to the anomalous Hall effect. However, ρ_{xy} is linear with magnetic field down to 10 K in the present crystal; the anomalous Hall effect is not applicable here to interpret the upturn of R_H. The upturn of R_H may suggest either some localization of charge carrier at low temperature in spite of the metallic $\rho_{ab}(T)$ down to 2 K or reduction of density of states at the Fermi surface because of some unknown factors.

Figure 6 shows the temperature dependence of the thermoelectric power (TEP). The value of TEP at room temperature is $\approx +110$ μV K^{-1}, as large as that in $Na_{0.75}CoO_2$. However, $[Bi_2Ba_{1.3}K_{0.6}Co_{0.1}O_4]^{RS}[CoO_2]_{1.97}$ has larger resistivity than that of $Na_{0.75}CoO_2$ [18]. TEP decreases with decreasing temperature. The calculated power factor $Q = S^2/\rho$ is 3.2×10^{-4} W m^{-1} K^{-2}, larger than those observed in $Bi_2Ca_2Co_2O_y$ ($\approx 2.7 \times 10^{-4}$ W m^{-1} K^{-2}) and $Ca_3Co_4O_9$ ($\approx 1.8 \times 10^{-4}$ W m^{-1} K^{-2}) single crystals [19]. Q increases to 6.5×10^{-4} W m^{-1} K^{-2} at around 100 K

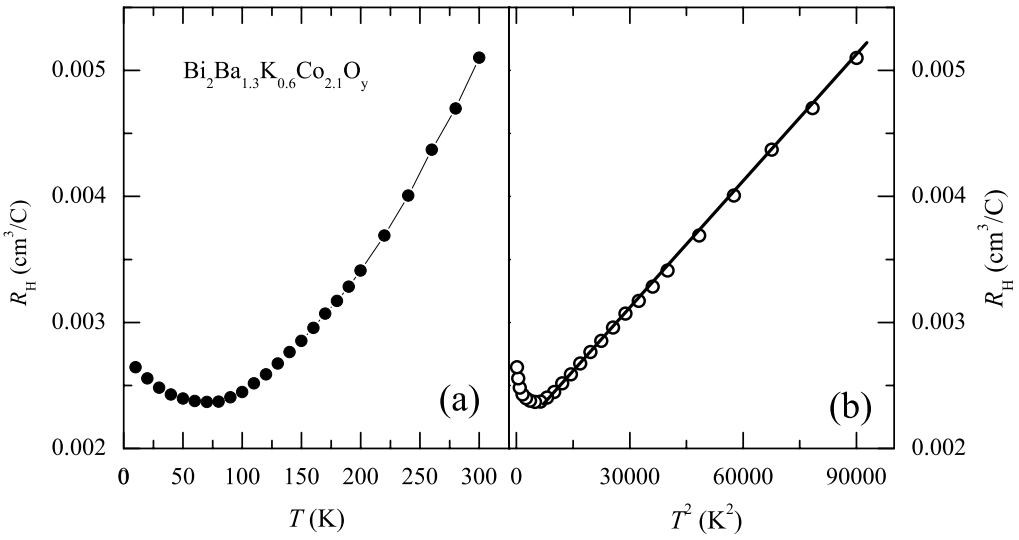

Figure 5. Temperature dependence of the Hall coefficient for the $[Bi_2Ba_{1.3}K_{0.6}Co_{0.1}O_4]^{RS}[CoO_2]_{1.97}$ single crystal. (b) The square T dependence of the Hall coefficient.

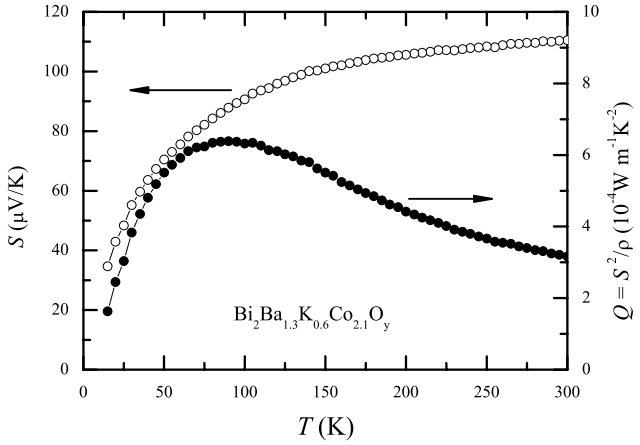

Figure 6. Temperature dependence of thermoelectric power (TEP) and power factor for $[Bi_2Ba_{1.3}K_{0.6}Co_{0.1}O_4]^{RS}[CoO_2]_{1.97}$ single crystal.

and then decreases with decreasing temperature. This maximum is much larger than the obtained maximum of Q in $Bi_2Ca_2Co_2O_y$ ($\approx 3.2 \times 10^{-4}$ W m^{-1} K^{-2}) and $Ca_3Co_4O_9$ ($\approx 2.1 \times 10^{-4}$ W m^{-1} K^{-2}) single crystals [19]. This indicates that the $[Bi_2Ba_{1.3}K_{0.6}Co_{0.1}O_4]^{RS}[CoO_2]_{1.97}$ single crystal has a better thermoelectric performance than the $Bi_2Ca_2Co_2O_y$ and $Ca_3Co_4O_9$ single crystals [19]. But the thermoelectric performance of the $[Bi_2Ba_{1.3}K_{0.6}Co_{0.1}O_4]^{RS}[CoO_2]_{1.97}$ single crystal is lower than those observed in Na_xCoO_2 ($x \geqslant 0.70$) according to the data reported by Lee *et al* [18].

3.4. Magnetotransport

Figure 7 shows the temperature dependence of in-plane resistivity under different magnetic fields (H) varying from 0 to 14 T. A striking feature is observed that magnetic field leads to a transition from metallic to semiconductor-like behavior at low temperature with H both perpendicular and parallel to the ab plane. The minimum resistivity appears in $\rho_{ab}(T)$ and obvious positive MR is observed. As shown in figure 9, the temperature corresponding to the minimum resistivity shifts to high temperature with increasing magnetic field. At 2.5 K and 8 T, the positive MR reaches 4% when H lies in the ab plane and 6% when H is along the c-axis, respectively. These values are much lower than that observed in the undoped polycrystalline sample, where about 10% of MR was observed at 2.5 and 7 T [12]. The effect of H on $\rho_{ab}(T)$ is stronger with $H \parallel ab$ plane than with $H \perp ab$ plane. As shown in figure 8, a similar effect of H on $\rho_c(T)$ is also observed. Although the upturn of $\rho_c(T)$ at low temperature follows a thermal activation behavior without magnetic field, external magnetic field leads to a change of low-temperature resistivity from a thermal activation behavior to a $\ln(1/T)$ diverging behavior with H both perpendicular and parallel to the ab plane. This suggests that $\rho_{ab}(T)$ and $\rho_c(T)$ show the same temperature dependence under H at low temperature, although they show contrasting behavior (metallic in $\rho_{ab}(T)$ and semiconducting in $\rho_c(T)$) without H.

Figure 9 shows the magnetic field dependence of the temperature corresponding to the minimum resistivity ($\rho_{ab}(T)$

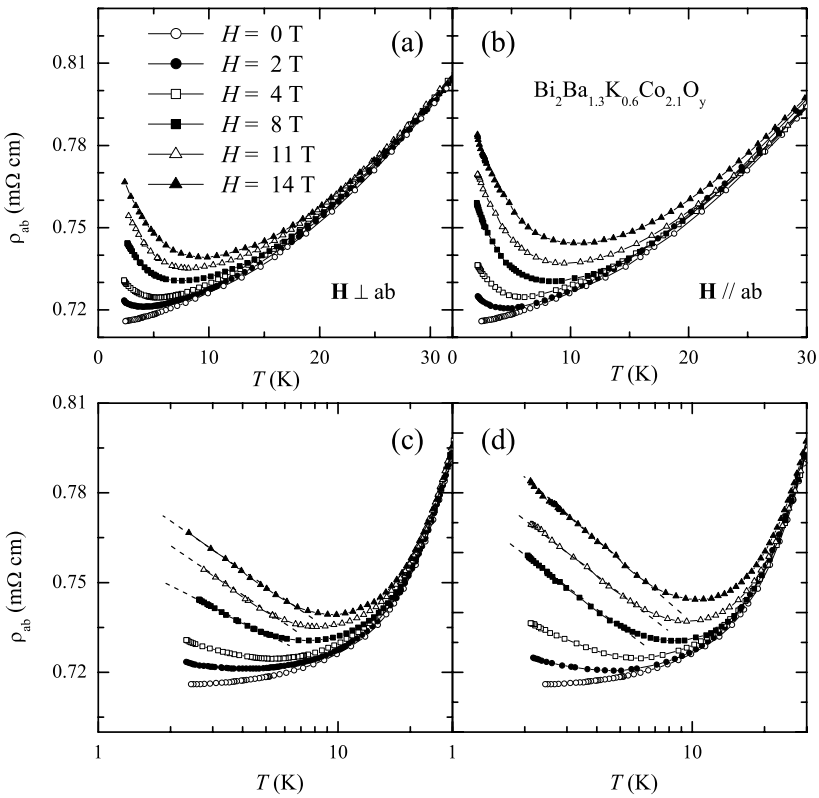

Figure 7. Temperature dependence of in-plane magnetoresistivity under different magnetic fields (a) perpendicular and (b) parallel to the ab plane for the $[Bi_2Ba_{1.3}K_{0.6}Co_{0.1}O_4]^{RS}[CoO_2]_{1.97}$ single crystal. (c) and (d) are replots of (a) and (b) in a $\log(T)$ scale, respectively. The dashed lines guide the eyes, linear in $\ln(1/T)$.

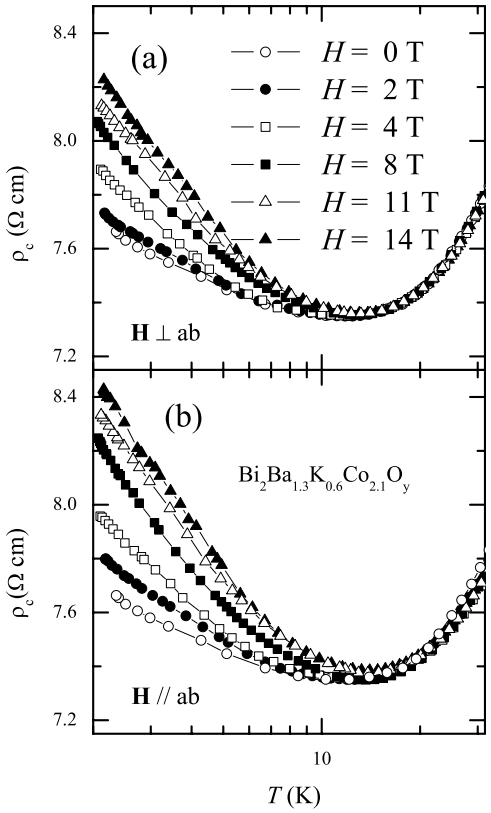

Figure 8. Temperature dependence of out-of-plane magnetoresistivity under different magnetic fields (a) perpendicular and (b) parallel to the *ab* plane for the $[Bi_2Ba_{1.3}K_{0.6}Co_{0.1}O_4]^{RS}[CoO_2]_{1.97}$ single crystal.

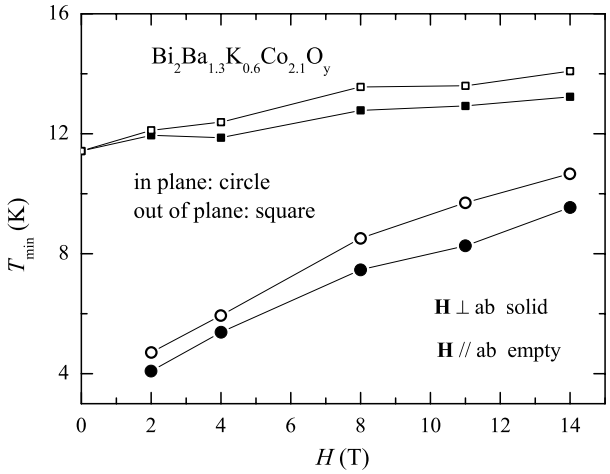

Figure 9. The temperature corresponding to the minimum $\rho_{ab}(T)$ and $\rho_c(T)$ as a function of magnetic field with H parallel and perpendicular to the *ab* plane for the $[Bi_2Ba_{1.3}K_{0.6}Co_{0.1}O_4]^{RS}[CoO_2]_{1.97}$ single crystal.

and $\rho_c(T)$). It indicates that the temperature corresponding to the minimum resistivity (T_{min}) increases with increasing H, suggesting that the localization is enhanced by H. It should be pointed out that T_{min} in $\rho_c(T)$ is enhanced slightly with increasing magnetic field, contrasting to the strong dependence of T_{min} in $\rho_{ab}(T)$. Negative MR is a common feature in $Ca_3Co_4O_9$ and (Bi, Pb)$_2$M$_2$Co$_2$O$_y$ (M = Sr and Ca), in which semiconducting resistivity can usually be observed below a certain temperature [2, 6, 7], while with M = Ba large positive MR has been observed in a polycrystalline sample [12]. The negative MR has been explained to be related to the spin-dependent transport at temperatures below or close to the magnetic ordering transitions, while the positive MR is not clearly understood. In the previous reports, no such obvious positive MR has been found in *metallic* triangular cobaltites: either $Tl_{0.4}SrCoO_x$ or Na_xCoO_2. $Na_{0.75}CoO_2$ is an exceptional case; the spin density wave (SDW) has been taken into account for interpreting the anomalously large positive MR in it [20]. We tried to fit the $\rho_{ab}(T)$ at $H = 8$, 11 and 14 T below T_{min} with a variety of functional forms. It turned out that the resistivity at low temperature under H cannot be fitted by formulae including thermal activation ($\ln\rho \sim -1/T$), various types of variable range hopping (VRH) conduction ($\ln\rho \sim -T^{-\alpha}$ with $\alpha = \frac{1}{2}$, $\frac{1}{3}$ and $\frac{1}{4}$) and power law ($\ln\rho \sim \ln T$). Instead, the data at high magnetic field with H both perpendicular and parallel to the *ab* plane exhibit a $\ln(1/T)$ divergence ($\rho \sim \ln(1/T)$) as shown in figures 7(c), (d) and 8. Such magnetic-field-induced localization has not been observed in the triangular layered cobaltites previously.

The in-plane and out-of-plane isothermal MRs were measured at 5 and 10 K with H varying from 0 to 14 T as shown in figure 10. All the MRs are positive and increase with lowering temperature. The value of MR with $H \parallel ab$ is larger than that with $H \parallel c$ at a fixed temperature. The MR does not follow the classical H^2 law or Kohler's law (i.e. collapsing to a single curve in the Kohler plot, $\delta\rho/\rho$ versus H/ρ_0). The MRs do not follow a linear relationship to H, as claimed by Hervieu *et al* in the undoped polycrystalline sample [12]. These unusual positive MRs may be related to the magnetic-field-induced localization as indicated in figures 7 and 8.

4. Discussion and conclusions

Magnetotransport behavior can usually be related to the Fermi surface [21]. For example, a square Fermi surface can lead to a linear MR due to the presence of sharp corners [21]. For systems with multiband electronic structure involving two types of charge carriers, the H dependence of MR can be written as

$$\Delta\rho/\rho(0) = aH^2/(b + cH^2) \quad (1)$$

where a, b and c are positive, H-independent quantities determined by the relaxation rates of each type of charge carrier [22]. We tried to fit the MR data shown in figure 10 using equation (1). Surprisingly, the out-of-plane MR data can be well fitted using equation (1), as shown in figure 8. The in-plane MR data can also be roughly fitted. Therefore, the isothermal MR could suggest the multiband electronic structure in the $[Bi_2Ba_{1.3}K_{0.6}Co_{0.1}O_4]^{RS}[CoO_2]_{1.97}$ single crystal. Local density approximation (LDA) calculations in $NaCo_2O_4$ predicted a large cylindrical Fermi surface around the Γ–A line, surrounding by small satellite hole-like pockets centered about two-thirds of the way out on the Γ–K and A–H directions [23]. In Na_xCoO_2, however, no such satellite

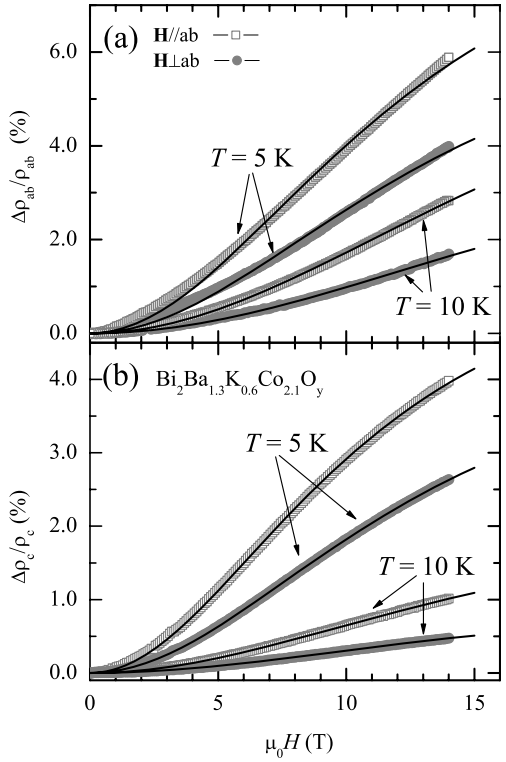

Figure 10. Magnetic field dependence of the in-plane and out-of-plane isothermal MR with H parallel and perpendicular to the ab plane for the $[Bi_2Ba_{1.3}K_{0.6}Co_{0.1}O_4]^{RS}[CoO_2]_{1.97}$ single crystal. The solid lines are the fitting results with equation (1).

hole-like pocket has been experimentally observed [24]. From another point of view, because of the peculiar rhombohedral coordination the t_{2g} orbitals of the low-spin Co^{3+} and Co^{4+} in the triangular cobaltites would be split, forming heavy a_{1g} and light e'_g holes [23, 25]. This may be used to interpret the MR.

Slight deviation from equation (1) is observed for the in-plane isothermal MRs. Therefore, there could be some other mechanisms for this positive MR in addition to the multiband electronic structure. A magnetic-field-induced logarithmic temperature dependence of in-plane resistivity has been observed, as shown in figures 7(c) and (d). Such magnetic-field-induced logarithmic temperature-dependent resistivity has been reported in high-T_c cuprates, in which the logarithmically temperature-dependent resistivity appears when superconductivity is suppressed by external magnetic field [26]. There are two main points of view to interpret such logarithmic resistivity. In cuprates, the *field-induced* SDW state has been taken as one of the points of view to interpret the logarithmically temperature-dependent resistivity [27–29]. In most misfit-layered triangular cobaltites, such as $Ca_3Co_4O_9$, $(Bi, Pb)_2M_2Co_2O_y$ (M = Ca and Sr), the SDW is a common spin ordered state [10]. Determining from the μSR results, however, no SDW exists down to 1.8 K at zero or low field in undoped $Bi_2Ba_2Co_2O_y$ [10], with large positive MR at low temperature. But from the magnetic data, however, the SDW probably exists in the present crystal and thus the field-enhanced SDW may be taken as one candidate to explain the logarithmically temperature-dependent resistivity in magnetic field. Up to now, however, no evidence for the field-enhanced SDW has been reported in triangular cobaltites. Consequently, μSR experiments could be desired to establish whether the SDW exists in the present compound and if it can be enhanced by magnetic field.

Another point of view is the weak localization in 2D systems [30, 31], which theoretically predicts a logarithmic temperature dependence of the conductivity [32]. The misfit structure leads the system to be two-dimensional structurally. The large anisotropy and the strong temperature dependence of the anisotropy as shown in figure 2 suggests the $[Bi_2Ba_{1.3}K_{0.6}Co_{0.1}O_4]^{RS}[CoO_2]_{1.97}$ single crystal to be a (quasi-) 2D electronic system. From these results, it is also possible that field-induced 2D weak localization results in the logarithmically temperature-dependent resistivity. This is the reason why the in-plane MR data are roughly fitted with slight deviation based on the multiband electronic structure with two types of charge carriers.

In conclusion, the electrical transport properties have been systematically studied for the $[Bi_2Ba_{1.3}K_{0.6}Co_{0.1}O_4]^{RS}$ $[CoO_2]_{1.97}$ single crystal. An anomalous behavior is observed in that there exists a contrasting behavior at low temperature in the in-plane resistivity ($\rho_{ab}(T)$) and out of plane ($\rho_c(T)$): metallic behavior down to 2 K with a T^2 dependence below 30 K in $\rho_{ab}(T)$; while a thermal activation semiconducting behavior below about 12 K in $\rho_c(T)$. Magnetic field leads to a $\ln(1/T)$ diverging behavior in both ρ_{ab} and $\rho_c(T)$ at low temperature. The isothermal out-of-plane MR can be quite well fitted by taking into account the multiband electronic structure with two types of charge carriers. The $\ln(1/T)$ diverging $\rho_{ab}(T)$ in magnetic field could arise from the field-enhanced 2D weak localization or magnetic-field-induced spin density wave.

Acknowledgments

This work is supported by the National Natural Science Foundation of China and by the Ministry of Science and Technology of China (973 project Nos 2006CB601001 and 2006CB0L1205).

References

[1] Terasaki I, Sasago Y and Uchinokura K 1997 *Phys. Rev.* B **56** R12685
[2] Masset A C, Michel C, Maignan A, Hervieu M, Toulemonde O, Studer F and Raveau B 2000 *Phys. Rev.* B **62** 166
[3] Wang Y Y, Rogado N S, Cava R J and Ong N P 2003 *Nature* **423** 425 (*Preprint* cond-mat/0305455)
[4] Li S Y, Taillefer L, Hawthorn D G, Tanatar M A, Paglione J, Sutherland M, Hill R W, Wang C H and Chen X H 2004 *Phys. Rev. Lett.* **93** 056401
[5] Takada K, Sakurai H, Takayama-Muromachi E, Izumi F, Dilanian R A and Sasaki T 2003 *Nature* **422** 53
[6] Yamamoto T, Tsukada I, Takagi M, Tsubone T and Uchinokura K 2001 *J. Magn. Magn. Mater.* **226–230** 2031
Yamamoto T, Uchinokura K and Tsukada I 2002 *Phys. Rev.* B **65** 184434
[7] Maignan A, Hebert S, Hervieu M, Machel C, Pelloquin D and Khomskii D 2003 *J. Phys.: Condens. Matter* **15** 2711

[8] Foo M L, Wang Y Y, Watauchi S, Zandbergen H W, He T, Cava R J and Ong N P 2004 *Phys. Rev. Lett.* **92** 247001
[9] Wang C H, Chen X H, Wu T, Luo X G, Wang G Y and Luo J L 2006 *Phys. Rev. Lett.* **96** 216401
[10] Sugiyama J, Brewer J H, Ansaldo E J, Itahara H, Tani T, Mikami M, Mori Y, Sasaki T, Hebert S and Maignan A 2004 *Phys. Rev. Lett.* **92** 017602
[11] Leligny H, Grebille D, Perez O, Masset A C, Hervieu M, Michel C and Raveau B 1999 *C. R. Acad. Sci. Paris* II **2** 409
Leligny H, Grebille D, Perez O, Masset A C, Hervieu M, Michel C and Raveau B 2000 *Acta Crystallogr.* B **56** 173
[12] Hervieu M, Maignan A, Michel C, Hardy V, Creon N and Raveau B 2003 *Phys. Rev.* B **67** 045112
[13] Luo X G, Chen X H, Wang G Y, Wang C H, Li X, Miao W J, Wu G and Xiong Y M 2006 *Eur. Phys. J.* B **49** 37
[14] Shannon R D 1976 *Acta Crystallogr.* A **32** 751
Shannon R D and Prewitt C T 1969 *Acta Crystallogr.* B **25** 925
[15] Valla T, Johnson P D, Yusof Z, Wells B, Li Q, Loureiro S M, Cava R J, Mikami M, Mori Y, Yoshimura M and Sasaki T 2002 *Nature* **417** 627
Yusof Z, Wells B O, Valla T, Johnson P D, Fedorov A V, Li Q, Loureiro S M and Cava R J 2006 *Preprint* cond-mat/0610271
[16] Chen X H, Yu M, Ruan K Q, Li S Y, Gui Z, Zhang G C and Cao L Z 1998 *Phys. Rev.* B **58** 14219
[17] Luo X G, Chen X H, Wang C H, Wang G Y, Xiong Y M, Song H B, Li H and Lu X X 2006 *Europhys. Lett.* **74** 526
[18] Lee M, Viciu L, Li L, Wang Y Y, Foo M L, Watauchi S, Pascal R A Jr, Cava R J and Ong N P 2006 *Nat. Mater.* **425** 537
[19] Luo X G, Jing Y C, Chen H and Chen X H 2008 *J. Cryst. Growth* **308** 309
[20] Motohashi T, Ueda R, Naujalis E, Tojo T, Terasaki I, Atake T, Karppinen M and Yamauchi H 2003 *Phys. Rev.* B **67** 064406
[21] Pippard A B 1989 *Magnetoresistance in Metal* (Cambridge: Cambridge University Press)
[22] Ziman J M 1972 *Principles of the Theory of Solids* 2nd edn (Cambridge: Cambridge University Press)
[23] Singh D J 2000 *Phys. Rev.* B **61** 13397
[24] Hasan M Z, Chuang Y D, Qian D, Li Y W, Kong Y, Kuprin A, Fedorov A V, Kimmerling R, Rotenberg E, Rossnagel K, Hussain Z, Koh H, Rogado N S, Foo M L and Cava R J 2004 *Phys. Rev. Lett.* **92** 246402
[25] Mizokawa T, Tjung L H, Steeneker P G, Brookes N B, Tsukada I, Yamamoto T and Uchinokura K 2001 *Phys. Rev.* B **64** 115104
[26] Ando Y, Boebinger G S, Passner A, Kimura T and Kishio K 1995 *Phys. Rev. Lett.* **75** 4662
[27] Sun X F, Komiya S, Takeya J and Ando Y 2003 *Phys. Rev. Lett.* **90** 117004
[28] Komiya S and Ando Y 2004 *Phys. Rev.* B **70** 060503
[29] Luo X G, Chen X H, Liu X, Wang R T, Wang C H, Huang L, Wang L and Xiong Y M 2005 *Supercond. Sci. Technol.* **18** 234
[30] Hidaka Y, Yamaji Y, Sugiyama K, Tomiyama F, Yamagishi A, Date M and Hikita M 1991 *J. Phys. Soc. Japan* **60** 1185
[31] Hagen S J, Xu X Q, Jiang W, Peng J L, Li Z Y and Greene R L 1992 *Phys. Rev.* B **45** 515
[32] Bergmann G 1984 *Phys. Rep.* **107** 1